Study of the influence of nuclear spin and dilution over the slow relaxation in a 3d4f heterobimetallic single-molecule magnet

Jessica Flores Gonzalez, Bertrand Lefeuvre, Bastien Degraeve, Olivier Cador, Fabrice Pointillart

Study of the nuclear spin and dilution influence over the slow relaxation in a 3d4f heterobimetallic Single-Molecule Magnet

Received 00th January 20xx,
Accepted 00th January 20xx

DOI: 10.1039/x0xx00000x

www.rsc.org/

Jessica Flores González[a], Bertrand Lefeuvre[a], Bastien Degraeve[a], Olivier Cador[a]*, Fabrice Pointillart[a]*

The effect of the isotopic enrichment and magnetic dilution has been investigated in an heterobimetallic complex of formula $[Zn_2L_2{}^{A}DyCl_3]\cdot 2H_2O$ (**$^{A}DyZn_2$**) (A=162 and 163) presenting slow relaxation of the magnetization. The isotopic substitution for ^{162}Dy (I=0) and ^{163}Dy (I=5/2) leads to a shift in the relaxation times depending on the suppression or favor of the hyperfine interactions. The release of the dipolar interactions through magnetic dilution in an Y(III)-based matrix, enhances the slow relaxation of the magnetization and the visibility of the nuclear spin effect. A comparison of the hysteresis loop at 0.5 K for bulk and diluted analogues of pure isotopically enriched complexes suggested a role of the nuclear spin in the interaction between the active system and the matrix.

Introduction

The single molecule magnets are in scope since 1993, with the first publication of a molecular entity displaying magnetic bistability.[1] Since, an increased interest of these kind of properties is produced due to their potential applications in the high-density data storage[2] and spintronic devices[3]. In this kind of complexes, the magnetic bistability results from the appearance of an anisotropic barrier, responsible of the slow relaxation at low temperature. In this sense, mononuclear complexes based on lanthanides have been extensively studied because of their large magnetic moments, high intrinsic magnetic anisotropy and a bistable ground state under appropriate conditions. In order to achieve this requisites, some strategies have been studied: on one side, the optimization of the coordination environment (symmetry and crystal field) to enhance a large splitting of the ground multiplet state. This has recently driven researchers to create molecules achieving open hysteresis up to 60 K[4] and later 80 K[5]; on the other side, the minimization of the dipolar and hyperfine interactions which interfere in the relaxation process, enhancing some through-barrier relaxations. This second block, includes the isolation of the paramagnetic centres (by frozen solution[6], doping in a diamagnetic matrix[7] or even inclusion of diamagnetic divalent ions in the structure (M=Co(II), Zn(II)[8-10]) to study the contribution of the environment, and the isotopic enrichment of the magnetic centre in order to have a better insight of the contribution of its own nuclear spin (I)[11-15].

In the lasts ten years, different groups have considered the effect of the isotopic enrichment of Ln(III) in order to tune the relaxation of the magnetization. In 2010, F. Luis *et al.*[11] studied the isotopic effect of the first Er-based SMM enriched with ^{167}Er(III) (I=7/2). Some of us reported in 2015[12a] the isotopic effect in a Dy-based SMM with two different isotopes (^{161}Dy (I=5/2) and ^{164}Dy (I=0)) and showed that the magnetization relaxation slows down for nuclear spin silent isotopes in the quantum regime. This study was extended in 2019 with the investigations of the four main stable isotopes of the same system[12b], showing the difference between two isotopes with the same I=5/2 nuclear spin. More recent publications have argued the importance of this isotopic effect in other Dy-based systems[13,14] and for the first time in 2021 similar effect was demonstrated for the prolate Yb(III)[15].

Until now, Dy- and Yb-based systems tend to show a common magnetic behavior consisting in the slowing down of the relaxation when suppressing the nuclear spin and the acceleration with nuclear spin active analogues, in the quantum regime only.[12-15] This tendency is opposite to polyoxometallate Er-based system proposed by F. Luis *et al.*[11]. These opposite tendencies have not yet been elucidated and the question remains open.

Heterobinuclear 3d-4f systems, resulted from the two-step complexation of a divalent diamagnetic metal ion, Zn(II), and a Lanthanide cation with a Schiff base ligand, have been reported in the literature to show good SMM performances.[9-10] These systems, enable the inclusion of a divalent diamagnetic Zn(II) ion in the second coordination sphere of the metal, polarizing the phenoxido oxygen atoms and favouring an axial distribution of the electron density, which enhances the SMM behavior.

In this paper, we propose to go a step further in the magnetic study of a mononuclear lanthanide based Zn-Dy-Zn type SMM formed by the salen-type ligand H_2L (H_2L=N, N'-bis(3-methoxysalicylidene)phenylene-1,2-diamine), previously studied by W.-B. Sun *et al.* in 2016 (hereafter abbreviated as **$DyZn_2$**)[10]. Indeed, this system fulfils certain requirements: i) it involves a magnetically isolated Dy(III) ion preventing any intramolecular magnetic interaction able to cancel the isotopic effect,[14a] ii) the maxima of the out-of-phase component of the magnetic susceptibility are centred in the experimental frequency windows (0.1-1500 Hz) and iii) the system is easy to synthetize and well-known in a magnetic point of view. Thus, the isotopic enrichment and the dilution in an isomorphous diamagnetic matrix have been coupled in order to study the different contributions to the relaxation mechanism.

Materials and methods

Single crystals of **$DyZn_2$**, **$^{162}DyZn_2$**, **$^{163}DyZn_2$**, (**Dy@Y)Zn_2**, (**^{162}Dy@Y)Zn_2** and (**^{163}Dy@Y)Zn_2** were mounted on a APEXIII D8 VENTURE Bruker-AXS diffractometer for cell measurements (MoK_α radiation source, λ=0.71073 Å, T=150 K) in the "Centre de Diffractométrie X" (CDIFX), University of Rennes 1, France. X-ray diffraction (XRD) patterns were recorded at room temperature in the 2θ range 5-30° with a step size of 0.026° and a scan time per step of 600 s using a PANalytical X'Pert Pro

[a] *Univ Rennes, CNRS, ISCR (Institut des Sciences Chimiques de Rennes) - UMR 6226, F-35000 Rennes, France.*

† Electronic Supplementary Information (ESI) available: See DOI: 10.1039/x0xx00000x

diffractometer (Cu-L2,L3 radiation, λ=1.5418 Å, 40 kV, 40 mA, PIXcel 1D detector). Data collector and HighScore Plus softwares were used, respectively, for recording and analysis of the patterns. The Dy/Y ratio of the compounds (**^{162}Dy@Y)Zn$_2$**, **(Dy@Y)Zn$_2$** and **(^{163}Dy@Y)Zn$_2$** was determined using SEM (Scanning Electron Microscopy). All observations and measurements were carried out with a JEOL JSM 6400 scanning electron microscope (JEOL Ltd, Tokyo, Japan) with an EDS (Energy Dispersive Spectrometry) analysis system (Oxford Link INCA). The voltage was kept at 9 kV, and the samples were mounted on carbon stubs and coated for 5 min with a gold/palladium alloy using a sputter coater (Jeol JFC 1100). These analyses were performed by the "Centre de Microscopie Electronique à Balayage et microAnalyse (CMEBA)" from the University of Rennes 1 (France).

The *ac* and *dc* magnetic susceptibility measurements were performed on solid polycrystalline samples with a Quantum Design MPMS-XL SQUID magnetometer equipped with iQuantum He3 insert. The sample was immobilized in a pellet made with Teflon tape. These measurements were corrected for the diamagnetic contribution as calculated with Pascal's constants.

Experimental

The isotopically enriched Dy_2O_3 oxides are commercially available from Eurisotop Company and Innova-Chem SAS. All other reagents were purchased from Sigma-Aldrich Co. Ltd and were used without further purification.

$[Zn_2L_2{}^ADyCl_3]\cdot 2H_2O]$ (**^{A}DyZn$_2$**) complexes with L=N,N'-bis(3-methoxysalicylidene)phenylene-1,2-diamine and A=162 and 163, were synthesized following a modified version of an already published procedure.[10,16]

Isotopically enriched $^ADyCl_3\cdot 6H_2O$ were formed by dissolving 50 mg of $^ADy_2O_3\cdot 6H_2O$, enriched at 94.40 % for A=162 and at 92.8 % for A=163, in 130 µL of 37% HCl. After 30 minutes at 60°C with continuous stirring, the resulting solution was diluted with 1 mL of distilled water and let evaporated giving $^ADyCl_3\cdot 6H_2O$ which can be used without further purification. A $^ADyCl_3\cdot 6H_2O$ (12-13.1 mg, 0.03 mmol) solution in 10 mL of methanol was added to a suspension solution of Zn(N,N'-bis(3-methoxysalicylidene)phenylene-1,2-diamine), previously synthesized following a reported procedure.[10] (27-28 mg, 0.06 mmol) in the same volume of acetonitrile. The mixture was first stirred and heated under reflux for 6 h, and then filtered after cooling it to room temperature. The resulted solution was distributed into different tubes and crystallization took place by diffusion of diethyl ether in a sealed container. Yields from isolated single crystals: **DyZn$_2$**: 4 mg (11%); **^{162}DyZn$_2$**: 4.8 mg (13%); **^{163}DyZn$_2$**: 4 mg (11%). Anal. Calcd (%) for $C_{44}H_{36}Cl_3DyN_4O_{10}Zn_2$: C 44.62, H 3.40, N 4.73; found: C 44.59, H 3.31, N 4.70; Anal. Calcd (%) for $C_{44}H_{36}Cl_3{}^{162}DyN_4O_{10}Zn_2$: C 44.62, H 3.40, N 4.73; found: C 44.55, H 3.29, N 4.69; Anal. Calcd (%) for $C_{44}H_{36}Cl_3{}^{163}DyN_4O_{10}Zn_2$: C 44.62, H 3.40, N 4.73; found: C 44.66, H 3.34, N 4.68. IR (cm^{-1}): **DyZn$_2$**: 3053(w), 3029(w), 2974(m), 2940(m), 2881(m), 2839(w), 1735(w), 1613(s), 1586(m), 1551(m), 1453(s), 1393(m), 1304(m), 1281(m), 1233(s), 1195(s), 1097(m), 1073(m), 1049(m), 969(m), 882(m), 846(m), 782(m), 741(s), 648(w), 631(w), 559(m), 511(m), 445(w); **^{162}DyZn$_2$**: 3060(w), 3029(w), 2936(w), 2841(w), 1733(w), 1613(s), 1587(m), 1552(m), 1457(s), 1392(m), 1234(s), 1194(s), 1098(m), 1073(w), 969(m), 848(m), 783(m), 742(s), 649(w), 633(w), 559(m), 512(m), 447(w); **^{163}DyZn$_2$**: 3058(w), 3029(w), 2974(w), 2935(w), 2839(w), 1612(s), 1587(m), 1551(m), 1453(s), 1392(m), 1301(w), 1281(m), 1235(s), 1196(s), 1097(m), 1071(m), 1044(w), 968(m), 848(m), 783(m), 742(s), 649(w), 633(w), 560(m), 510(m), 446(w).

$[Zn_2L_2(^ADy_{0.1}Y_{0.9})Cl_3]\cdot 2H_2O$, **(^{A}Dy@Y)Zn$_2$**, have been prepared with the same protocol but starting with $^ADyCl_3\cdot 6H_2O$ (6 mg, 0.015 mmol) and $YCl_3\cdot 6H_2O$ (43.3-43.5 mg, 0.14 mmol) dissolved in methanol (50 mL) and added to a suspension solution of Zn (N,N'-bis(3-methoxysalicylidene)phenylene-1,2-diamine) (135 mg, 0.3 mmol) in the same volume of acetonitrile. Calculated yields from isolated single crystals: **(Dy@Y)Zn$_2$**: 29.5 mg (17.2%); **(^{162}Dy@Y)Zn$_2$**: 10.6 mg (6%); **(^{163}Dy@Y)Zn$_2$**: 30.1 mg (16.9%). IR: **(Dy@Y)Zn$_2$**: 3061(w), 3028(w), 2974(m), 2937(w), 2885(w), 2840(w), 1612(s), 1586(s), 1552(s), 1453(s), 1390(s), 1303(m), 1282(s), 1235(s), 1195(s); 1098(m), 1047(s), 968(m), 880(w), 848(m), 783(m), 739(s), 649(w), 634(w), 589(w), 560(m), 511(m), 447(w); **(^{162}Dy@Y)Zn$_2$**: 3053(w), 3030(w), 2973(m), 2937(m), 2889(m), 2842(w), 1614(s), 1586(s), 1552(s), 1453(s), 1392(s), 1302(m), 1282(s), 1234(s), 1194(s), 1097(m), 1073(m), 1047(m), 881(m), 847(m), 783(m), 742(s), 649(m), 632(w), 586(w), 559(m), 510(m), 446(w); **(^{163}Dy@Y)Zn$_2$**: 3062(w), 3028(w), 2972(m), 2936(m), 2888(m), 2840(w), 1614(s), 1586(s), 1552(s), 1450(s), 1391(s), 1303(m), 1282(s), 1236(s), 1195(s), 1168(m), 1097(s), 1047(s), 968(m), 882(m), 848(m), 782(m), 739(s), 650(m), 632(m), 588(w), 560(m), 512(m), 446(w).

Results and discussions

Structural description

The compounds **^{162}DyZn$_2$**, **^{163}DyZn$_2$**, **DyZn$_2$** and diluted **(^{162}Dy@Y)Zn$_2$**, **(^{163}Dy@Y)Zn$_2$**, **(Dy@Y)Zn$_2$** are isostructural (Table S1) to the previously published structure.[10] The phase purity of all the samples was checked by powder X-ray diffraction (Fig. S1). The ratio Dy/Y have been determined by EDS analyses: ^{162}Dy/Y:0.17/0.83, ^{163}Dy/Y:0.15/0.85 and Dy/Y:0.13/0.87. The crystal structure (Fig. 1) is briefly remembered hereafter. The ($N_2O_2O_2$) ligand enables a first coordination to a diamagnetic Zn(II) ion in the N_2O_2 pocket and a second one between the eight outer oxygen from two L moieties, in which the Dy(III) is encapsulated. The ninth coordination site of the Dy(III) centre is occupied with a Cl^- anion located on C_2 symmetry axis. The polarization effect driven by the two Zn(II) cations[9d], enhances the difference in the electronic density between the bridging oxygens (rich electron density) and those situated in the perpendicular plane (poor electron density), thus favouring an Ising axis of the magnetization pointing in the direction of the highest electron density.

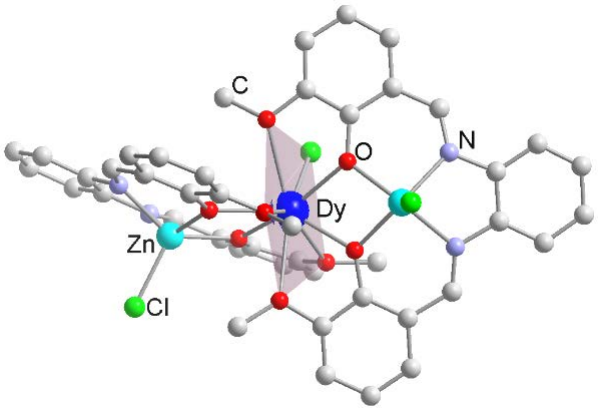

Fig. 1 Molecular structure of **$DyZn_2$**, with the hard plane represented. Hydrogen atoms and water molecules are omitted for clarity. Adapted from ref. [10].

Magnetic properties

The dynamic magnetic properties of the two isotopologues **$^{162}DyZn_2$** (I=0) (Fig. 2a, S2a and S3) and **$^{163}DyZn_2$** (I=5/2) (Fig. 2c, S2c and S4) are determined by measuring the frequency dependence of the magnetic susceptibility from 2 to 30 K, and have been compared to the natural isotope **$DyZn_2$** (Fig. 2b, S2b and S5). The last, reported in the literature,[10] has been re-measured in the same experimental condition than the two isotopologues for a better comparison. The out-of-phase components of the magnetic susceptibility for each compound pass through maxima at frequencies that depend on the isotopologue: at 2 K, it is centred at 0.4 Hz for **$^{162}DyZn_2$**, at 0.66 Hz for **$DyZn_2$** and 1 Hz for **$^{163}DyZn_2$**. The introduction of nuclear spin free ^{162}Dy(III) results into a shift of the out-of-phase component to lower frequencies (Fig. 2). The relaxation times (τ) for the different isotopologues at each temperature have been extracted from the extended Debye model (see the SI, Fig. S6, Tables S2-S4). The normalized Cole-Cole plots are depicted in Fig. S7-9 respectively for **$^{162}DyZn_2$**, **$^{163}DyZn_2$** and **$DyZn_2$** showing a typical semi-circle shape curves and demonstrating that almost the 100 % of the magnetization of the sample are slowly relaxing. The temperature dependence of the relaxation times (Fig. 3) follows an Orbach process at the highest temperatures with a visible deviation caused by the Raman process at the intermediate temperatures. Below 10 K the relaxation is dominated by a thermally-independent regime i.e. the Quantum Tunnelling of the Magnetization (QTM).[10,16] Based on the previous works, it is known that the thermally dependent Orbach and Raman processes should not be affected by the isotopic enrichment, thus the thermal variation of the relaxation time is simultaneously fitted for the three systems with the shared contribution of Orbach (Δ and τ_0) and Raman (C and n), and individual QTMs (τ_{TI}):

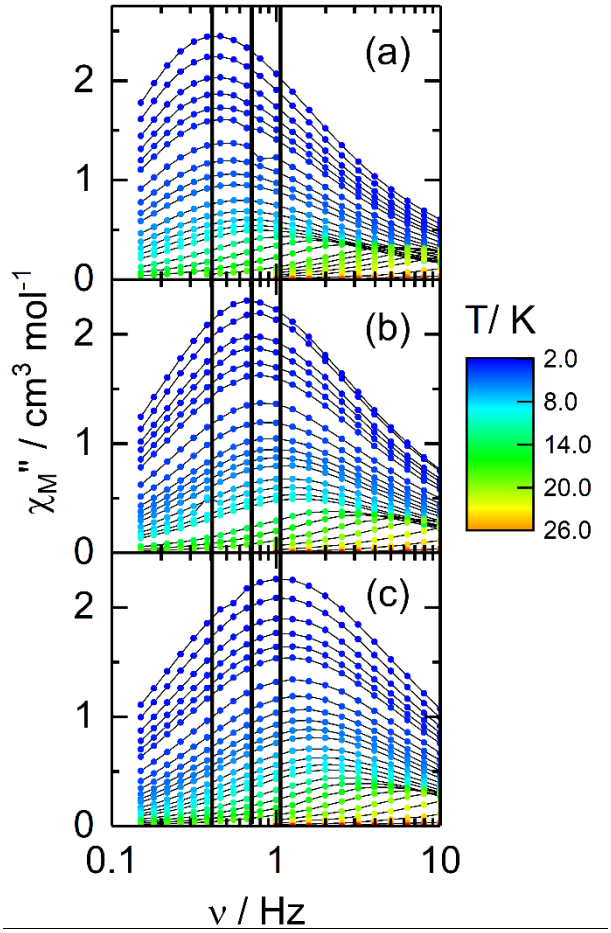

Fig. 2 Zoom of the frequency dependence (0.1 – 10 Hz) of the out-of-phase component of the ac susceptibility measured in zero dc field at various temperatures for a) **$^{162}DyZn_2$**, b) **$DyZn_2$** and c) **$^{163}DyZn_2$**.

$$\tau^{-1} = \tau_0^{-1} \exp(\Delta / T) + CT^n + \tau_{TI}$$

The value of n is initially 9 for Kramers ions[17] but can be found between 2 and 7[18] because of the presence of acoustic and optical phonons, and in some cases even lower.[19] The best fitted parameters for Orbach, Δ=374(21) K and τ_0=3(2)×10^{-10} s, and Raman, C=0.039(36) s^{-1}K^{-n} and n=3.0(3), are close to the previously reported[10]; with the addition of the QTM at lower temperatures (τ_{TI}(**$^{162}DyZn_2$**)=0.35(3) s; τ_{TI}(**$DyZn_2$**)=0.18(1) s and τ_{TI}(**$^{163}DyZn_2$**)=0.11(1) s). In order to have a better insight of the isotopic effect, the diluted **(^{A}Dy@Y)Zn_2** systems have been investigated. Indeed, our previous work on a mononuclear Dy(III) complex demonstrated that the isotopic effect can be partially hidden by the presence of dipolar interactions.[12b]

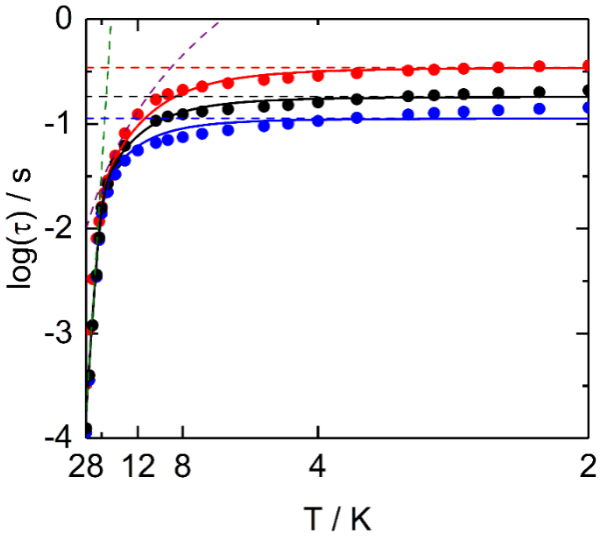

Fig. 3 Temperature dependence of the relaxation time of the magnetization for ^{162}**DyZn$_2$** (red), **DyZn$_2$** (black) and ^{163}**DyZn$_2$** (blue). Full lines are the best fitted curves, whereas the dashed lines refer to the Raman (purple), Orbach (green) and QTM (colour of the compound) contributions.

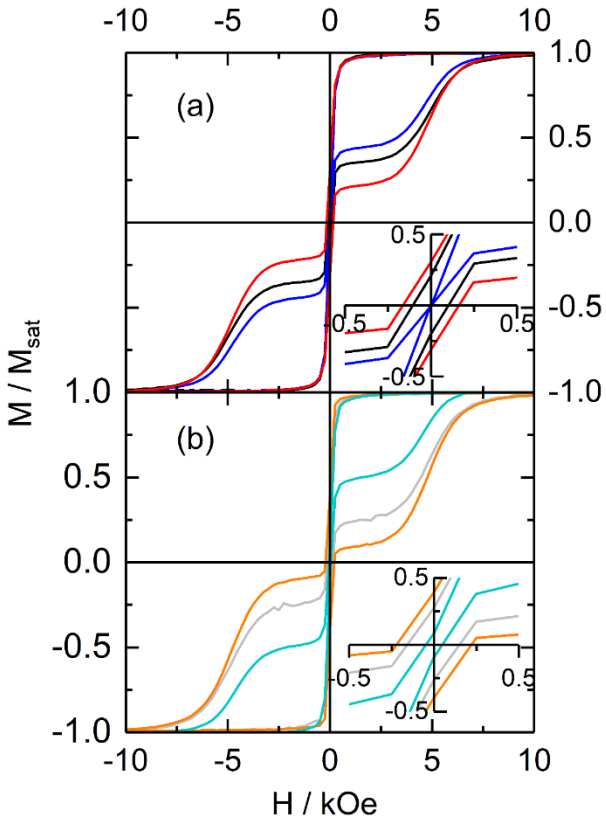

Fig. 4 Normalized magnetic hysteresis loops at 0.5 K and at a sweep rate of 16 Oe s^{-1} for (a) the condensed compounds **DyZn$_2$** (black), ^{162}**DyZn$_2$** (red) and ^{163}**DyZn$_2$** (blue); and (b) the diluted **(Dy@Y)Zn$_2$** (grey), **(^{162}Dy@Y)Zn$_2$** (orange) and **(^{163}Dy@Y)Zn$_2$** (light blue) analogues. The insets correspond to a zoomed view of the origin.

At 2 K, the out-of-phase component of the natural **(Dy@Y)Zn$_2$** led to a relaxation of the magnetization shifted out of the lowest frequency limit (Fig. S10) of the experimental window. Then, the comparison has been envisaged through the opening of the hysteresis loop at 0.5 K for the different diluted and concentrated compounds. As predicted by the ac properties, the original butterfly shaped hysteresis loop is open at zero field for both **DyZn$_2$** and ^{162}**DyZn$_2$** whereas it is closed for the nuclear spin active ^{163}**DyZn$_2$** (Fig. 4a). Moreover the observed coercive field (H_c) trend is ^{162}**DyZn$_2$** (H_c=329 Oe)>**DyZn$_2$** (H_c=203 Oe)>^{163}**DyZn$_2$** (H_c=0 Oe) and comforts the isotopic enrichment effect observed on the magnetic relaxation in zero field for T<12 K (Fig. 3). The fast relaxation coming from dipolar interactions is minimized on dilution and the hysteresis loops continue to open (Fig. 4b). One should mention larger coercive field for diluted samples than for the bulk ones with the measured values of 436 Oe, 320 Oe and 99 Oe for **(^{162}Dy@Y)Zn$_2$**, **(Dy@Y)Zn$_2$** and **(^{163}Dy@Y)Zn$_2$** respectively.

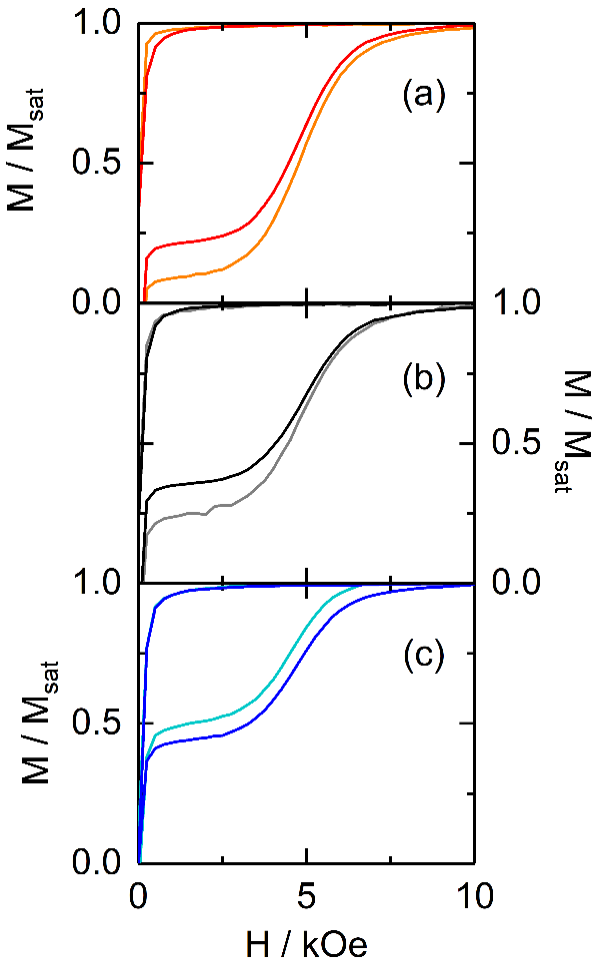

Fig. 5 Zoom of the positive section of the normalized magnetic hysteresis loops at 0.5 K and at a sweep rate of 16 Oe s^{-1} for the condensed and diluted samples of (a) ^{162}Dy-(**^{162}DyZn$_2$** (red) and (**^{162}Dy@Y)Zn$_2$** (orange)), (b) Dy-(**DyZn$_2$** (black) and **(Dy@Y)Zn$_2$** (grey)) and (c) ^{163}Dy-(**^{163}DyZn$_2$** (blue) and (**^{163}Dy@Y)Zn$_2$** (light blue)) based systems analogues.

Moreover, these differences in the hysteresis loops are not only visible at zero field but also in-field (*i.e.* the wings of the butterfly) for both dilution and enrichment (Fig. 4, 5 and S11). The pure nuclear spin active isotopologues **(^{163}Dy@Y)Zn$_2$** and ^{163}**DyZn$_2$** are characterized by smaller gap between upper and lower branches of the loops in-field compared with the nuclear spin free and the natural analogues, thus endorsing the reported idea of a greater probability of relaxation paths and interaction with the matrix (phonons bath) because of the greater number of sublevels coming from the splitting of the

I=5/2 in eight states under the hyperfine coupling.[14c] In order to prove the role of the M_J levels in this opening, and discard the diffusion of the zero field memory in field, we determined gaps (δ_1, δ_2 and δ_3, Fig. S12) in magnetization between two isotopologues at the same magnetic field (1.25 kOe) and compared them to the same gaps at zero field. δ_1, δ_2 and δ_3 increase respectively of 38%, 15% and 29 % from 0 Oe to 1.25 kOe (Table S5). Such differences of hysteresis loops between the different isotopologues were already observed by some of us in a Dy(III) mononuclear complex.[12a] To support the hypothesis of stronger interaction with the matrix in case of the pure ^{163}Dy isotope (I=5/2), one could remark that for both natural and nuclear spin free isotopes, the hysteresis loops are more open for the diluted samples between 0 and 10 kOe (Fig. 5a and 5b) while the reverse trend is observed for ^{163}Dy (Fig. 5c and S10).

Conclusions

The Single Molecule Magnet properties of the two ^{162}Dy(III) and ^{163}Dy(III) isotopes have been investigated in the $DyZn_2$ system. The nuclear spin free isotope (**$^{162}DyZn_2$**) displayed a slightly slower magnetic relaxation than the nuclear spin active **$^{163}DyZn_2$** because of the suppression of the hyperfine interactions effect coming from the metal centre. Thus, demonstrating that the isotopic enrichment effect on the magnetic relaxation in a hetero-bimetallic complex followed the same trend than already observed in pure lanthanide complex. By magnetic dilution, the dipolar interactions were suppressed leading to a slowing down of the magnetic relaxation rate which could be observed by means of the hysteresis loop. Finally, the comparison of the different hysteresis for diluted samples make us point to an isotopic effect in zero field as already proven in other systems, but also that we may consider that this has some effect under applied magnetic field which might be due to the interaction between the M_J sublevels and the matrix.

Conflicts of interest

There are no conflicts to declare.

Acknowledgements

This work was supported by CNRS, Université de Rennes and the European Research Council through the ERC-CoG 725184 MULTIPROSMM (project n. 725184).

Notes and references

1 R. Sessoli, D. Gatteschi, A. Caneschi and M. A. Novak, *Nature*, 1993, **365**, 141.

2 D. Gatteschi, R. Sessoli and J. Villain, Molecular Nanomagnets, Oxford University Press, 2006.

3 S. Thiele, F. Balestro, R. Ballou, S. Klyatskaya, M. Ruben and W. Wernsdorfer, *Science*, 2014, **344**, 1135–1138.

4 a) C. A. P. Goodwin, F. Ortu, D. Reta, N. F. Chilton and D. P. Mills, *Nature*, 2017, **548**, 439–442; b) F.-S. Guo, B. M. Day, Y.-C. Chen, M.-L. Tong, A. Mansikkamäki, R. A. Layfield, *Angew. Chem. Int. Ed.,* 2017, **56**, 11445–11449.

5 F.-S. Guo, B. M. Day, Y.-C. Chen, M.-L. Tong, A. Mansikkamäki and R. A. Layfield, *Science*, 2018, **362**, 1400–1403.

6 G. Cosquer, F. Pointillart, S. Golhen, O. Cador and L. Ouahab, *Chem. – Eur. J.*, 2013, **19**, 7895–7903.

7 F. Habib, P. H. Lin, J. Long, I. Korobkov, W. Wernsdorfer and M. Murugesu, *J. Am. Chem. Soc.*, 2011, **133**, 8830– 8833.

8 a) X. Lü, W. Bi, W. Chai, J. Song, J. Meng, W.-Y. Wong, W.-K. Wong and R. A. Jones, *New. J. Chem.,* 2008, **32**, 127–131; b) J. L. Liu, Y. C. Chen, Y. Z. Zheng, W. Q. Lin, L. Ungur, W. Wernsdorfer, L. F. Chibotaru and M. L. Tong, *Chem. Sci.*, 2013, **4**, 3310–3316; c) S. K. Langley, N. F. Chilton, L. Ungur, B. Moubaraki, L. F. Chibotaru and K. S. Murray, *Inorg. Chem.*, 2012, **51**, 11873–11881; d) S. K. Langley, N. F. Chilton, B. Moubaraki and K. S. Murray, *Chem. Commun.*, 2013, **49**, 6965–6967.

9 a) J. Long, R. Vallat, R. A. S. Ferreira, L. D. Carlos, F. A. Almeida Paz, Y. Guari and J. Larionova, *Chem. Commun.,* 2012, **48**, 9974–9976; b) A. Upadhyay, S. K. Singh, C. Das, R. Mondol, S. K. Langley,K. S. Murray, G. Rajaraman and M. Shanmugam, *Chem. Commun.*, 2014, **50**, 8838–8841; c) J. Long, E. Mamontova, V. Freitas, D. Luneau, V. Vieru, L. F. Chibotaru, R. A. S. Ferreira, G. Félix, Y. Guari, L. D. Carlos and J. Larionova, *RSC Adv.*, 2016, **6**, 108810–108818; d) A. Upadhyay, C. Das, S. Vaidya, S. K. Singh, T. Gupta, R. Mondol, S. K. Langley, K. S. Murray, G. Rajaraman and M. Shanmugam, *Chem. Eur. J.*, 2017, **23**, 4903–4916; e) A.-L. Boulkedid, J. Long, C. Beghidja, Y. Guari, A. Beghidja and J. Larionova, *Dalton Trans*, 2018, **47**, 1402–1406.

10 W.-B. Sun, P.-F. Yan, S.-D. Jiang, B.-W. Wang, Y.-Q. Zhang, H.-F. Li,P. Chen, Z.-M. Wang and S. Gao, *Chem. Sci.*, 2016, **7**, 684–691.

11 F. Luis, M. J. Martínez-Pérez, O. Montero, E. Coronado, S. Cardona-Serra, C. Martí-Gastaldo, J. M. Clemente-Juan, J. Sesé, D. Drung and T. Schurig, *Phys. Rev. B*, 2010, **82**, 060403(R).

12 a) F. Pointillart, K. Bernot, S. Golhen, B. Le Guennic, T. Guizouarn, L. Ouahab and O. Cador, *Angew. Chem. Int. Ed.*, 2015, **54**, 1504–1507; b) J. Flores Gonzalez, F. Pointillart and O. Cador, *Inorg. Chem. Front.*, 2019, **6**, 1081–1086.

13 a) Y. Kishi, F. Pointillart, B. Lefeuvre, F. Riobé, B. Le Guennic, S. Golhen, O. Cador, O. Maury, H. Fujiwara and L. Ouahab, *Chem. Commun.*, 2017, **53**, 3575–3578; b) L. Tesi, Z. Salman, I. Cimatti, F. Pointillart, K. Bernot, M. Mannini and R. Sessoli, *Chem. Commun.*, 2018, **54**, 7826–7829.

14 a) G. Huang, X. Yi, Julien Jung, O. Guillou, O. Cador, F. Pointillart, B. Le Guennic and K. Bernot, *Eur. J. Inorg. Chem.*, 2018, 326–332; b) F. Ortu, D. Reta, Y.-S. Ding, C. A. P. Goodwin, M. P. Gregson, E. J. L. McInnes, R. E. P. Winpenny, Y.-Z. Zheng, S. T. Liddle, D. P. Mills and N. F. Chilton, *Dalton Trans.*, 2019, **48**, 8541–8545; c) E. Moreno-Pineda, G. Taran, W. Wernsdorfer and M. Ruben, *Chem. Sci.*, 2019, **10**, 5138–5145.

15 J. Flores Gonzalez, H. Douib, B. Le Guennic, F. Pointillart and O. Cador, *Inorg. Chem.*, 2021, **2**, 540–544.

16 W.-K. Lo, W.-K. Wong, W.-Y. Wong, J. Guo, K.-T. Yeung, Y.-K. Cheng, X. Yang and R. A. Jones, *Inorg. Chem.*, 2006, **45**, 9315–9325.

17 A. Abragam, and B. Bleaney, *Electron Paramagnetic Resonance of Transition Ions*, Clarendon Press: Oxford, **1970**.

18 a) A. Singh and K. N. Shrivastava, *Phys. Status Solidi B,* 1979, **95**, 273; b) K. N. Shirivastava, *Phys. Status Solidi B,* 1983, **177**, 437.

19 a) P. Evans, D. Reta, G. F. S. Whitehead, N. F. Chilton and D. P. Mills, *J. Am. Chem. Soc.*, 2019, **141**, 19935-19940; b) D. Reta and N. F. Chilton, *Phys. Chem. Chem. Phys.*, 2019, **21**, 23567-23575.